

Non-reactive scattering of excited exotic hydrogen atoms)*

G.Ya. Korenman, V.P. Popov and V.N. Pomerantsev
Institute of Nuclear Physics, Moscow State University

Abstract

The Coulomb deexcitation of light exotic atoms in collisions with hydrogen atoms has been studied in the framework of the fully quantum-mechanical close-coupling method for the first time. The calculations of the l -averaged cross sections have been performed for $(\mu p)_n$ and $(\mu d)_n$ atoms in the states with the principal quantum number $n = 3 \div 8$ and relative energies region $E = 0.01 \div 100$ eV. The obtained results reveal the new n and E dependences of the Coulomb deexcitation cross sections. The large fraction (up to $\sim 36\%$) of the transition with $\Delta n > 1$ is also predicted.

1 Introduction

In this paper we present *ab initio* quantum-mechanical treatment of non-reactive scattering processes of the excited exotic hydrogen-like atoms:

- elastic scattering

$$(ax)_n + (be^-)_\nu \rightarrow (ax)_n + (be^-)_\nu; \quad (1)$$

- Stark mixing

$$(ax)_{nl} + (be^-)_\nu \rightarrow (ax)_{nl'} + (be^-)_\nu; \quad (2)$$

- Coulomb deexcitation

$$(ax)_{nl} + (be^-)_\nu \rightarrow (ax)_{n'l'} + (b^- e)_\nu. \quad (3)$$

Here $(a, b) = (p, d, t)$ are hydrogen isotopes and $x = \mu^-, \pi^-, K^-, \tilde{p}$; (n, l) are the principal and orbital quantum numbers of exotic atom and ν are the hydrogen atom quantum numbers. The processes (1) - (2) decelerate while Coulomb deexcitation (3) accelerates the exotic atoms, influencing their quantum number and energy distributions during the cascade. The last process has attracted particular attention especially after the "hot" πp atoms with the kinetic energy up to 200 eV were found experimentally [1,2].

Starting from the classical paper by Leon and Bethe [3], Stark transitions has been treated in the semiclassical straight-line-trajectory approximation (see [4] and references therein). The fully quantum-mechanical treatment of the processes (1) - (2) based on the adiabatic description was given in [5-8]. Recently [9,10], the elastic scattering and Stark transitions have also been studied in a close-coupling approach with the electron screening effect taken into account by the model.

*The work was supported by Russian Foundation for Basic Research (grant No. 03-02-16616).

Thus, at the present time we have more or less realistic description of the processes (1)-(2) in a wide range of n and E .

Concerning the acceleration process (3), the situation here is much less defined, especially for low n . The first work (to the best of our knowledge) on the CD process was performed by Bracci and Fiorentini [11] using the semiclassical approach with some additional approximations concerning the assumption of the large values of the quantum numbers under consideration ($n \gg 3$) and some others. In the following numerous papers [12, 13] (and references therein) the CD process is considered within the asymptotic approaches using the adiabatic hidden crossing theory [14] for the pure Coulomb three-body systems or for the screened Coulomb centers chosen in the static form (the dipole screening). Recently, the calculations of the process (3) were also performed in the classical-trajectory Monte-Carlo (CTMC) [15] approach. While the Coulomb deexcitation cross sections obtained in CTMC approach are in fair agreement with the semiclassical ones of Bracci and Fiorentini [11], the much more elaborated advanced adiabatic approach (AAA) [12,13] gives much smaller Coulomb deexcitation cross sections which can not explain the experimental data. The reasons of such a strong discrepancy are not clear. One can only assume that the semiclassical model [11] as well as the CTMC approach are not valid for low-lying states. Thus, until now there is no satisfactory description of this process in the most interesting region ($n = 3 \div 7$).

The main aim of this paper is to obtain the cross sections of Coulomb deexcitation for $3 \leq n \leq 8$ in realistic quantum-mechanical approach which is free from the additional approximations used in previous studies, in particular, the two-state approximation. For this reason we use a unified treatment of elastic scattering, Stark transitions and Coulomb deexcitation within the close-coupling method. This approach was used previously for the study of the elastic scattering and Stark transitions of the excited muonic hydrogen in the collisions with the hydrogen ones [16] and a good agreement as compared with the results of the quantum-mechanical adiabatic description [5-8] was obtained. In the following section we briefly describe the close-coupling formalism and the main expressions. The results of the close-coupling calculations concerning the total cross sections of the process (3) are presented and discussed in Sec. III. Finally, summary and concluding remarks are given in Sec. IV.

2 Theory

The non-relativistic Hamiltonian for the four-body system ($a\mu^- + b e^-$), after separating the center of mass motion, can be written in Jacobi coordinates $(\mathbf{R}, \boldsymbol{\rho}, \mathbf{r})$ as

$$H = -\frac{1}{2m}\Delta_{\mathbf{R}} + h_{\mu}(\boldsymbol{\rho}) + h_e(\mathbf{r}) + V(\mathbf{r}, \boldsymbol{\rho}, \mathbf{R}), \quad (4)$$

where m is the reduced mass of the system, V is the electrostatic interaction between the subsystems, h_{μ} and h_e are the Hamiltonian of the free exotic and hydrogen atoms

$$h_{\mu}\Phi_{nlm}(\boldsymbol{\rho}) = \varepsilon_n\Phi_{nlm}(\boldsymbol{\rho}), \quad (5)$$

$$h_e\varphi_{1s}(\mathbf{r}) = \epsilon_{1s}\varphi_{1s}(\mathbf{r}), \quad (6)$$

where $\Phi_{nlm}(\boldsymbol{\rho})$ and $\varphi_{1s}(\mathbf{r})$ are the wave functions of the exotic atom and hydrogen atom bound states, ε_n and ϵ_{1s} are the corresponding eigenvalues. The interaction potential of the subsystems is defined by

$$V(\mathbf{r}, \boldsymbol{\rho}, \mathbf{R}) = V_{ab} + V_{ub} + V_{ae} + V_{ue} \quad (7)$$

with the two-body Coulomb interactions

$$V_{ab} = \frac{1}{r_{ab}} = |\mathbf{R} + \nu \boldsymbol{\rho} - \nu_e \mathbf{r}|^{-1}, V_{\mu b} = -\frac{1}{r_{\mu b}} = -|\mathbf{R} - \xi \boldsymbol{\rho} - \nu_e \mathbf{r}|^{-1}, \quad (8)$$

$$V_{\mu e} = \frac{1}{r_{\mu e}} = |\mathbf{R} - \xi \boldsymbol{\rho} + \xi_e \mathbf{r}|^{-1}, V_{ae} = -\frac{1}{r_{ae}} = -|\mathbf{R} + \nu \boldsymbol{\rho} + \xi_e \mathbf{r}|^{-1}. \quad (9)$$

Here we use the set of Jacobi coordinates $(\mathbf{R}, \boldsymbol{\rho}, \mathbf{r})$:

$$\mathbf{R} = \mathbf{R}_H - \mathbf{R}_{\mu a}, \quad \boldsymbol{\rho} = \mathbf{r}_\mu - \mathbf{r}_a, \quad \mathbf{r} = \mathbf{r}_e - \mathbf{r}_b,$$

where $\mathbf{r}_a, \mathbf{r}_b, \mathbf{r}_\mu, \mathbf{r}_e$ are the radius-vectors of the nuclei, muon and electron in the lab-system, $\mathbf{R}_H, \mathbf{R}_{\mu a}$ are the center of mass radius-vectors of the hydrogen and exotic atoms, respectively. The coefficients ν, ξ, ν_e and ξ_e in the two-body interactions (8)-(9) depend on the masses of the particles,

$$\nu = m_\mu / (m_\mu + m_a), \quad \xi = m_a / (m_\mu + m_a), \quad (10)$$

$$\nu_e = m_e / (m_e + m_b), \quad \xi_e = m_b / (m_e + m_b), \quad (11)$$

and satisfy

$$\nu + \xi = \nu_e + \xi_e = 1. \quad (12)$$

$(m_a, m_b, m_\mu$ and m_e are the masses of the hydrogen isotopes, muon and electron, respectively). Atomic units (a.u) $\hbar = e = m_e m_b / (m_e + m_b) = 1$ will be used throughout the paper unless otherwise stated.

The total wave function $\Psi(\boldsymbol{\rho}, \mathbf{r}, \mathbf{R})$ of the system satisfies the time independent Schrödinger equation with the Hamiltonian (4):

$$(-\frac{1}{2m} \Delta_{\mathbf{R}} + h_\mu + h_e + V) \Psi(\boldsymbol{\rho}, \mathbf{r}, \mathbf{R}) = E \Psi(\boldsymbol{\rho}, \mathbf{r}, \mathbf{R}), \quad (13)$$

where E is the total energy of the system.

In this paper, as well as in the previous studies [11, 12, 15], we assume that the state of the target electron is fixed during the collision. The electron excitations can be taken into account in a straightforward manner. Owing to the rotation and inversion symmetries of the total system, the vector solutions of (13) is introduced the total angular momentum representation. In a space-fixed coordinate frame we built the basis states from the eigenvectors of the operators $h_e, h_\mu, \mathbf{l}^2, \mathbf{L}^2, \mathbf{J}^2, J_z$ and the total parity π with eigenvalues $\varepsilon_{1s}, \varepsilon_n, l(l+1), L(L+1), J(J+1), M$ and $(-1)^{l+L}$, respectively:

$$|\Gamma\rangle \equiv \phi_{1s}(\mathbf{r}) |\gamma\rangle \quad (14)$$

where

$$|\gamma\rangle \equiv |nl, L : JM\rangle \equiv i^L \sum_{m\lambda} \langle lmL\lambda | JM \rangle \Phi_{nlm}(\boldsymbol{\rho}) Y_{L\lambda}(\hat{\mathbf{R}}), \quad (15)$$

$$|\Gamma\rangle \equiv \frac{1}{\sqrt{4\pi}} R_{1s}(r) R_{nl}(\rho) \mathcal{Y}_{lL}^{JM}(\hat{\boldsymbol{\rho}}, \hat{\mathbf{R}}), \quad (16)$$

$$\mathcal{Y}_{lL}^{JM}(\hat{\boldsymbol{\rho}}, \hat{\mathbf{R}}) \equiv i^{l+L} \sum_{m\lambda} \langle lmL\lambda | JM \rangle Y_{lm}(\hat{\boldsymbol{\rho}}) Y_{L\lambda}(\hat{\mathbf{R}}) \quad (17)$$

Here the orbital angular momentum \mathbf{l} of $(a\mu)_{nl}$ is coupled with the orbital momentum \mathbf{L} of the relative motion to give the total angular momentum, $\mathbf{J} = \mathbf{l} + \mathbf{L}$. Then, for the fixed values of $J, M, \pi = (-1)^{l+L}$ the exact solution of the Schrödinger equation for the colliding system,

$$(E - H)\Psi_E^{JM\pi}(\mathbf{r}, \boldsymbol{\rho}, \mathbf{R}) = 0, \quad (18)$$

is expanded as follows

$$\Psi_E^{JM\pi}(\mathbf{r}, \boldsymbol{\rho}, \mathbf{R}) = \varphi_{1s}(\mathbf{r}) \frac{1}{R} \sum_{nlL} G_{nlL}^{J\pi}(R) |nl, L : JM\rangle, \quad (19)$$

where the $G_{nlL}^{J\pi}(R)$ are the radial channel functions and the sum is restricted to (l, L) values to satisfy the total parity conservation. This expansion leads to the coupled radial scattering equations

$$\left(\frac{d^2}{dR^2} + k_n^2 - \frac{L(L+1)}{R^2} \right) G_{nlL}^{J\pi}(R) = 2m \sum_{n'l'L'} W_{nlL, n'l'L'}^J(R) G_{n'l'L'}^{J\pi}(R), \quad (20)$$

where $k_n^2 = 2m(E - \varepsilon_n - \epsilon_{1s}) = 2m(E_{cm} + \Delta\varepsilon_{nn'})$ specify the channel wave numbers; E_{cm} is the relative motion energy in the entrance channel, $\Delta\varepsilon_{nn'} = 0.5\mu(n^2 - (n')^2)/(nn')^2$ is the difference of the exotic atom bound energies in the initial and the final states, μ is the reduced mass of the exotic atom. Finally, $W_{nlL, n'l'L'}^J$ are the matrix elements that couple asymptotic channels $(nl; J)$ and $(n'l'L'; J)$:

$$W_{nlL, n'l'L'}^J \equiv \langle 1s, nl, L : J | \hat{V} | 1s, n'l', L' : J \rangle. \quad (21)$$

The radial functions $G_{E, n'l'L'}^{J\pi}(R)$ must be regular everywhere, and, at $R \rightarrow 0$

$$G_{E, n'l'L'}^{J\pi}(0) = 0 (\sim R^{L+1}) \quad (22)$$

and at asymptotic distances ($R \rightarrow \infty$) satisfy the usual boundary conditions

$$G_{E, n'l'L'}^{J\pi}(R) \Rightarrow \frac{1}{\sqrt{k_f}} \{ \delta_{if} \delta_{nn'} \delta_{ll'} \delta_{LL'} e^{-i(k_i R - L\pi/2)} - S^J(nl, L \rightarrow n'l', L') e^{i(k_f R - L'\pi/2)} \}, \quad (23)$$

where k_i, k_f are the wave numbers of initial and final channels and $S^J(nl, L \rightarrow n'l', L')$ is the scattering matrix in the total angular momentum representation. The indexes of the entrance channel and target electron state are omitted for brevity. The scattering amplitude for $nlm \rightarrow n'l'm'$ is defined by

$$f(nlmL \rightarrow n'l'm'L' | \mathbf{k}_i, k_f, \hat{\mathbf{R}}) = \frac{2\pi i}{\sqrt{k_i k_f}} \sum_{JMLL'\lambda\lambda'} i^{L'-L} \langle lmL\lambda | JM \rangle \langle l'm'L'\lambda' | JM \rangle \times \\ \times Y_{L\lambda}^*(\hat{\mathbf{k}}_i) Y_{L'\lambda'}(\hat{\mathbf{R}}) T^J(nlL \rightarrow n'l'L'), \quad (24)$$

where the transition matrix T^J used here is given by

$$T^J(nl, L \rightarrow n'l', L') = \delta_{nn'} \delta_{ll'} \delta_{LL'} \delta_{mm'} \delta_{\lambda\lambda'} - S^J(nl, L \rightarrow n'l', L'). \quad (25)$$

The matrix elements (21) of the interaction potential (7-9) are given by

$$W_{nlL, n'l'L'}^J(R) = \frac{1}{4\pi} \int d\mathbf{r} d\boldsymbol{\rho} d\hat{\mathbf{R}} R_{1s}^2(r) R_{nl}(\rho) R_{n'l'}(\rho) \\ \times (\mathcal{Y}_{lL}^{JM})^*(\hat{\boldsymbol{\rho}}, \hat{\mathbf{R}}) V(\mathbf{r}, \boldsymbol{\rho}, \mathbf{R}) \mathcal{Y}_{l'L'}^{JM}(\hat{\boldsymbol{\rho}}, \hat{\mathbf{R}}), \quad (26)$$

where the radial hydrogen-like wave functions are given explicitly by

$$R_{nl}(\rho) = N_{nl} \left(\frac{2\rho}{na} \right)^l \exp(-\rho/na) \sum_{q=0}^{n-l-1} S_q(n, l) \left(\frac{2\rho}{na} \right)^q \quad (27)$$

(a is the Bohr' radius of the exotic atom in a.u.) with

$$N_{nl} = \left(\frac{2}{na} \right)^{3/2} \left[\frac{(n+l)!(n-l-1)!}{2n} \right]^{1/2}, \quad (28)$$

$$S_q(n, l) = (-)^q \frac{1}{q!(n-l-1-q)!(2l+1+q)!}. \quad (29)$$

Averaging $V(\mathbf{r}, \boldsymbol{\rho}, \mathbf{R})$ in (26) over 1s-state of hydrogen atom we obtain

$$\begin{aligned} V(\mathbf{R}, \boldsymbol{\rho}) &= \frac{1}{4\pi} \int_0^\infty d\mathbf{r} R_{1s}^2(r) V(\mathbf{r}, \boldsymbol{\rho}, \mathbf{R}) = \\ &= \frac{1}{\xi_e} \{ U_{\nu, \xi_e}(\mathbf{R}, \boldsymbol{\rho}) - U_{-\xi, \xi_e}(\mathbf{R}, \boldsymbol{\rho}) \} - \frac{1}{\nu_e} \{ U_{\nu, \nu_e}(\mathbf{R}, \boldsymbol{\rho}) - U_{-\xi, \xi_e}(\mathbf{R}, \boldsymbol{\rho}) \}, \end{aligned} \quad (30)$$

where

$$U_{\alpha, \beta}(\mathbf{R}, \boldsymbol{\rho}) = (1 + \frac{\beta}{|\mathbf{R} + \alpha \boldsymbol{\rho}|}) e^{-\frac{2|\mathbf{R} + \alpha \boldsymbol{\rho}|}{\beta}} \equiv \lim_{x \rightarrow 1} \left(1 - \frac{1}{2} \frac{\partial}{\partial x} \right) \beta \frac{e^{-\frac{2x|\mathbf{R} + \alpha \boldsymbol{\rho}|}{\beta}}}{|\mathbf{R} + \alpha \boldsymbol{\rho}|}. \quad (31)$$

Using the additional theorem for the spherical Bessel functions

$$\begin{aligned} \frac{e^{-\lambda|\mathbf{R}_1 + \mathbf{r}_1|}}{|\mathbf{R}_1 + \mathbf{r}_1|} &= \frac{4\pi}{\sqrt{R_1 r_1}} \sum_{t\tau} (-1)^t Y_{t\tau}^*(\hat{\mathbf{R}}_1) Y_{t\tau}(\hat{\mathbf{r}}_1) \times \\ &\quad \times \left\{ K_{t+1/2}(\lambda R_1) I_{t+1/2}(\lambda r_1) \Big|_{r_1 < R_1} + I_{t+1/2}(\lambda R_1) K_{t+1/2}(\lambda r_1) \Big|_{r_1 > R_1} \right\} \end{aligned} \quad (32)$$

($I_p(x)$ and $K_p(x)$ are the modified spherical Bessel functions of the first and third kind) and substituting eqs.(30-32) into (26), we integrate over the angular variables. Furthermore, using the angular momentum algebra and integrating over ρ , we obtain:

$$\begin{aligned} W_{nlL, n'l'L'}^J(R) &= (-1)^{J+l+l'} i^{l'+L'-l-L} \sqrt{\hat{l}\hat{l}'\hat{L}\hat{L}'} \sum_{t=0}^{t_m} (l0l'0|t0)(L0L'0|t0) \left\{ \begin{array}{cccc} l & l' & t \\ L' & L & J \end{array} \right\} \times \\ &\quad \times \left\{ \frac{1}{\xi_e} [(-1)^t W_t(R, \nu, \xi_e; nl, n'l') - W_t(R, \xi, \xi_e; nl, n'l')] - \right. \\ &\quad \left. - \frac{1}{\nu_e} [(-1)^t W_t(R, \nu, \nu_e; nl, n'l') - W_t(R, \xi, \nu_e; nl, n'l')] \right\} \end{aligned} \quad (33)$$

(t_m is the maximum value of the allowed multipoles). Here the next definitions are used:

$$\begin{aligned} W_t(R, \alpha, \beta; nl, n'l') &= \mathcal{N}_{nl, n'l'} \sum_{m_1=0}^{n-l-1} S_{m_1}(n, l) \left(\frac{2n'}{n+n'} \right)^{m_1} \sum_{m_2=0}^{n'-l'-1} S_{m_2}(n', l') \left(\frac{2n}{n+n'} \right)^{m_2} \times \\ &\quad \times \left\{ H_t(z) J_1^{t,s}(z, \lambda(n, n', \alpha, \beta)) - h_t(z) J_2^{t,s}(z, \lambda(n, n', \alpha, \beta)) + \right. \\ &\quad \left. + F_t(z) J_3^{t,s}(z, \lambda(n, n', \alpha, \beta)) + f_t(z) J_4^{t,s}(z, \lambda(n, n', \alpha, \beta)) \right\}, \end{aligned} \quad (34)$$

where $z = 2R/\beta$, $s = l + l' + m_1 + m_2$, $\hat{L} \equiv 2L + 1$;

$$\mathcal{N}_{nl,n'l'} = \frac{1}{n+n'} \left(\frac{2n'}{n+n'} \right)^{l+1} \left(\frac{2n}{n+n'} \right)^{l'+1} \sqrt{(n+l)!(n-l-1)!(n'+l')!(n'-l'-1)}; \quad (35)$$

$$\lambda(n, n', \alpha, \beta) = \frac{2nn'}{n+n'} \frac{a\alpha}{\beta}; \quad (36)$$

$$H_t(x) = (1-2t)h_t(x) + xh_{t+1}(x); \quad (37)$$

$$F_t(x) = (1-2t)f_t(x) - xf_{t+1}(x). \quad (38)$$

The functions $h_t(y)$ and $f_t(y)$ are given by

$$h_t(y) \equiv \sqrt{\frac{2}{\pi y}} K_{t+1/2}(y) \quad (39)$$

and

$$f_t(y) \equiv \sqrt{\frac{\pi}{2y}} I_{t+1/2}(y). \quad (40)$$

The radial integrals $J_i^{t,s}(x, \lambda)$ are defined as follows:

$$J_1^{t,s}(x, \lambda) = \int_0^{x/\lambda} y^{s+2} e^{-y} f_t(\lambda y) dy, \quad (41)$$

$$J_2^{t,s}(x, \lambda) = \lambda J_1^{t+1,s+1}(x, \lambda), \quad (42)$$

$$J_3^{t,s}(x, \lambda) = \int_{x/\lambda}^{\infty} y^{s+2} e^{-y} h_t(\lambda y) dy, \quad (43)$$

$$J_4^{t,s}(x, \lambda) = \lambda J_3^{t+1,s+1}(x, \lambda) \quad (44)$$

and calculated analytically using the power series for the modified Bessel functions.

Finally, we give the explicit expressions for the cross sections to be discussed in this paper. The partial cross sections of the processes (1) - (3) for the transitions $nl \rightarrow n'l'$, averaging over an initial distribution of the degenerated substates and summed over the degenerate final substates, are given by

$$\sigma^J(nl \rightarrow n'l'; E) = \frac{\pi}{k_i^2} \frac{2J+1}{2l+1} \sum_{LL'} |T^J(nlL \rightarrow n'l'L')|^2. \quad (45)$$

The l -averaged partial cross sections for the transitions $n \rightarrow n'$ are then computed by summing over l and l' with the statistic factor $(2l+1)/n^2$:

$$\sigma_{n \rightarrow n'}^J(E) = \frac{\pi}{k_i^2} \frac{2J+1}{n^2} \sum_{l, l' LL'} |T^J(nlL \rightarrow n'l'L')|^2. \quad (46)$$

The total cross sections for the transition $n \rightarrow n'$ is obtained by summing the corresponding partial cross section over the total angular momentum J :

$$\sigma_{nn'}(E) = \sum_J \sigma_{nn'}^J(E). \quad (47)$$

For the discussion of the obtained results and the comparison of them with the other approaches we will also need the total cross section of Coulomb deexcitation including all transitions $n \rightarrow n'$ with $n' < n$:

$$\sigma_n^{\text{CD}}(E) = \sum_{n' < n} \sigma_{nn'}(E). \quad (48)$$

3 Results

The close-coupling method described in the previous Section has been used to obtain the cross sections for the collisions of the μ^-p and μ^-d atoms in excited states with hydrogen atoms. The present paper had at least two goals: first, to apply the fully quantum-mechanical approach for the study of the processes (1) - (3) and, second, to clear the validity of the energy and principle quantum number dependence of the Coulomb deexcitation cross sections used in literature and based on the semiclassical model [11]. So, we present here only a small part of our results. In particular, to illustrate some main features of the calculated cross sections, we discuss only the l -averaged CD cross sections. The detailed results of the calculations will be published elsewhere.

The coupled differential equations (20) are solved numerically using the Numerov method and with the real boundary conditions involving the K -matrix instead of S -matrix. The corresponding T -matrix can be calculated from equation

$$T = 2K(I - iK)^{-1} = 2K^2(1 + K^2)^{-1} - 2iK(1 + K^2)^{-1},$$

where I is the unit matrix. In the calculations we have taken into account all possible multipoles in the interaction potentials and all open channels with $n' \leq n$.

The close-coupling calculations have been carried out for the relative collision energies E_{cm} from 0.01 up to 100 eV and for the excited states with $n = 3 \div 8$. At all energies we take into account so many values of the total angular momentum J and the relative angular momentum L that all the inelastic cross sections were calculated with the accuracy not less than 0.1%.

Table 1: Dependence of the elastic and deexcitation cross sections $\sigma_{nn'}$ for $(\mu d)_n + \text{H}$ collisions at energy $E_{\text{cm}} = 0.1$ eV on the number t_m of terms included in the multipole expansion for the matrix elements (33).

t_m	σ_{66}	σ_{65}	σ_{64}	σ_{63}	σ_{62}	σ_{61}
1	54.70	2.36	0.20	0.012	0.0003	0.0000002
2	50.24	5.55	0.37	0.055	0.0052	0.000008
3	51.58	4.82	0.38	0.038	0.0176	0.000038
4	52.65	2.71	0.38	0.031	0.0177	0.000060
5	52.31	2.72	0.39	0.026	0.0277	0.000079
6	54.19	1.42	0.36	0.031	0.0295	0.000093
7	54.77	1.04	0.32	0.032	0.0279	0.000100
8	54.46	1.18	0.30	0.030	0.0270	0.000102
9	54.36	1.17	0.29	0.028	0.0269	0.000103
10	54.31	1.20	0.30	0.029	0.0271	0.000103

The results of the calculations are presented in Tables 1-3 and Figs. 1-6. The effects of the higher multipoles in the expansion of the interaction potentials are large (see Table 1). In contrast

to the elastic scattering and Stark transitions in which the “dipole” approximation ($t_m = 1$) gives practically the exact results, there is no case for the Coulomb deexcitation. Ignoring the higher multipoles would lead to the significant distortions of the cross sections. As it is seen from Table 1 the results are sharply varied in the top part of the table ($t_m = 1 \div 7$) and are practically unchanged in the bottom one ($t_m = 8 \div 10$). Thus, to provide the proper treatment of the Coulomb deexcitation all the multipoles in the expansion of the interaction potential must be taken into account.

In Fig. 1 we present the J dependence of the partial-wave cross sections $\sigma_{nn'}^J$ for $n = 7$ at three fixed energies 0.1, 2, and 50 eV. It is seen that a substantial part of the Coulomb cross sections comes from the partial waves with rather a low J (in comparison with the elastic and Stark mixing processes). It is worthwhile to note that for $n = 3$ the range of J values is much less, e.g. at relative energies 0.01, 2 and 100 eV we obtain $J_{\max}^{CD} = 7, 11, 15$ respectively, whereas for the elastic scattering we obtain $J_{\max} = 7, 60, 120$ for the same energies.

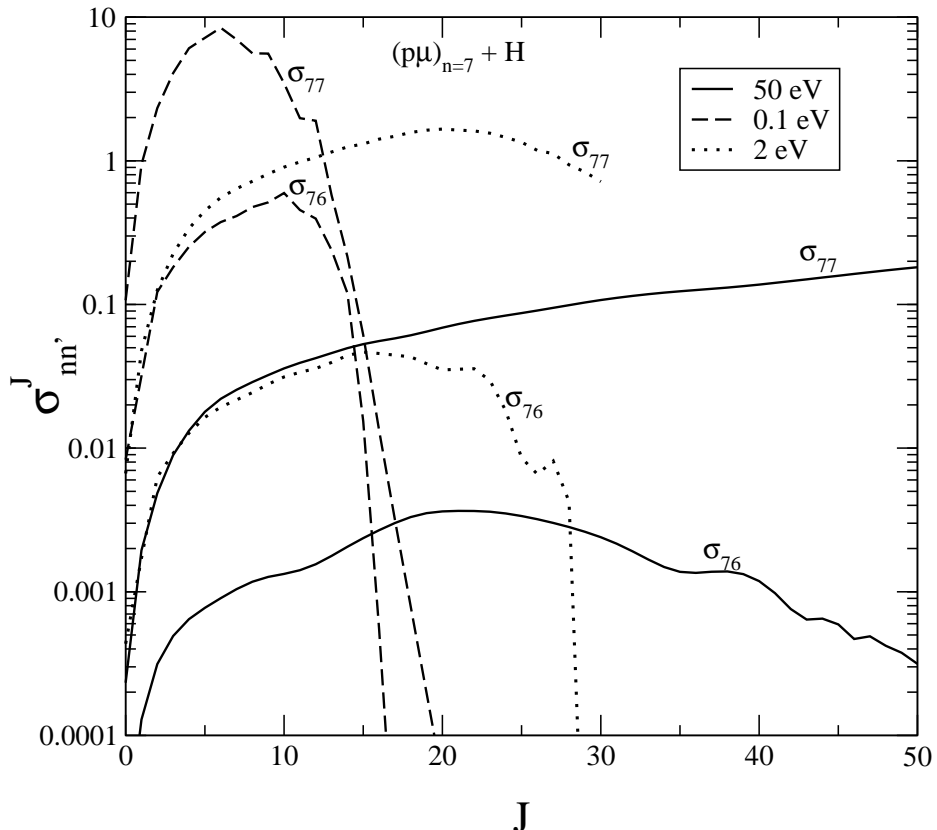


Figure 1: The partial cross sections of the Coulomb deexcitation $\sigma_{7,6}^J$ and the elastic scattering $\sigma_{7,7}^J$ in a.u. for $(\mu p)_{n=7} + H$ collisions as function of the total angular momentum J at three energies: 0.1 eV (dashed), 2 eV (dotted) and 50 eV (solid).

The convergence of the results upon the number of open channels (the transitions with $\Delta n > 1$ are included) is illustrated in Table 2 for $(\mu p)_{n=7} + D$ collisions at the relative energy $E_{\text{cm}} = 1$ eV. It is seen that only the nearest channels are most important. While n increasing the energy gap between the exotic atom states decreases. As a result the influence of the nearest channels becomes more significant and leads to the new n and E dependence of the Coulomb deexcitation cross sections as compared with the semiclassical ones.

The energy dependence of the total Coulomb deexcitation cross sections $\sigma_n^{CD}(E)$ for $n = 3 \div 8$

Table 2: The dependence of elastic and Coulomb deexcitation cross sections $\sigma_{7n'}$ for $(\mu p)_n + D$ collisions at energy $E_{cm} = 1$ eV on the number of open channels N_{level} included in the calculation (all terms of the multipole expansion for the potential are taken into account).

N_{level}	σ_{77}	σ_{76}	σ_{75}	σ_{74}	σ_{73}	σ_{72}	σ_{71}
2	39.578016	1.063412					
3	40.181324	0.679067	0.096652				
4	40.181170	0.598721	0.056935	0.009409			
5	40.177221	0.598219	0.055336	0.009368	0.001601		
6	40.177061	0.597370	0.055110	0.009343	0.001635	0.001241	
7	40.177065	0.597360	0.055110	0.009343	0.001635	0.001241	0.000005

is shown in Fig.2 in comparison with the results of Bracci and Fiorentini [11] for $n = 3, 5, 7$ and the CTMC calculations of Jensen and Markushin [15] for $n = 4 \div 8$ and $E_{cm} = 0.5$ and 5 eV. The present results are in poor agreement with the semiclassical results [11] and CTMC results [15]. There is only a qualitative agreement for $n = 5$ and energies above 2 eV. The energy dependence of the Coulomb deexcitation cross sections in our approach is approximately given by $1/\sqrt{E_{cm}}$ at $E_{cm} \lesssim 0.5$ eV (see Fig.3), in contrast to the $1/E_{cm}$ behavior found for low energies in [11] and also in the advanced adiabatic approach (AAA) [13].

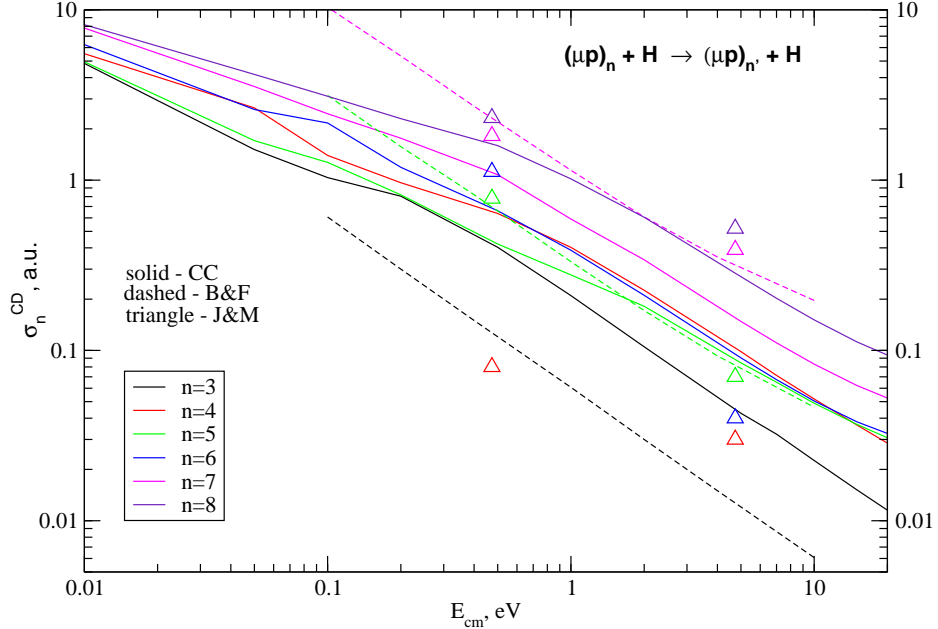


Figure 2: The cross sections of Coulomb deexcitation σ_n^{CD} in a.u. for $(\mu p)_n + H$ collisions calculated in the quantum-mechanical close-coupling method (solid lines) in comparison with the results of Bracci and Fiorentini [11] (dashed) and classic Monte-Carlo results [15] (triangles).

As for the n dependence of the total Coulomb deexcitation cross sections $\sigma_n^{CD}(E)$ the situation is more complicated than it is followed from the semiclassical model [11] (see Fig.2). There is no dependence $\sigma_n^{CD} \sim n^\gamma$ ($\gamma \sim 2$) as it is followed from [11]. Our prediction for the n dependence of the CD cross sections is quite different. In our opinion, this behaviour is explained by the

Table 3: The cross sections of Coulomb deexcitation for $(\mu p)_n + H$ collisions calculated in the quantum-mechanical close-coupling method.

E_{cm} , eV	0.01	0.05	0.1	0.2	0.5	1.0	2.0	5.0	7.0	10.0	15.0	20.0
$\sigma_{3,2}$	4.821	1.505	1.032	0.803	0.403	0.209	0.105	0.043	0.032	0.023	0.015	0.012
σ_3^{CD}	4.848	1.511	1.035	0.805	0.403	0.210	0.105	0.043	0.032	0.023	0.015	0.012
f_3 , %	0.6	0.4	0.3	0.2	0.2	0.2	0.2	0.2	0.2	0.2	0.2	0.2
$\sigma_{4,3}$	4.126	1.730	0.936	0.704	0.515	0.333	0.189	0.083	0.060	0.043	0.030	0.024
σ_4^{CD}	5.526	2.656	1.397	0.965	0.637	0.403	0.226	0.098	0.071	0.052	0.036	0.029
f_4 , %	25.3	34.9	33.0	27.0	19.1	17.2	16.4	16.0	16.2	16.3	16.5	16.7
$\sigma_{5,4}$	4.364	1.349	0.943	0.574	0.306	0.211	0.147	0.070	0.054	0.041	0.031	0.026
σ_5^{CD}	4.955	1.705	1.270	0.819	0.422	0.277	0.182	0.085	0.065	0.049	0.037	0.031
f_5 , %	11.9	20.9	25.8	30.0	27.4	23.9	19.0	17.2	16.5	16.1	15.4	14.9
$\sigma_{6,5}$	4.063	1.804	1.619	0.856	0.442	0.250	0.136	0.058	0.043	0.032	0.024	0.021
σ_6^{CD}	6.246	2.598	2.166	1.189	0.661	0.387	0.211	0.090	0.067	0.050	0.038	0.033
f_6 , %	35.0	30.6	25.3	28.0	33.1	35.4	35.5	36.0	36.5	36.8	36.8	36.1
$\sigma_{7,6}$	5.954	2.888	2.005	1.410	0.902	0.488	0.275	0.119	0.088	0.065	0.048	0.040
σ_7^{CD}	7.819	3.544	2.454	1.762	1.076	0.591	0.340	0.148	0.111	0.083	0.062	0.053
f_7 , %	23.9	18.5	18.3	20.0	16.2	17.5	19.3	19.9	20.4	21.2	22.3	23.4
$\sigma_{8,7}$	5.776	3.243	2.516	1.883	1.184	0.846	0.480	0.223	0.166	0.100	0.085	0.081
σ_8^{CD}	8.201	4.221	3.151	2.320	1.426	1.023	0.587	0.272	0.203	0.130	0.111	0.105
f_8 , %	29.6	23.2	20.1	18.8	17.0	17.3	18.1	17.9	18.0	23.3	23.0	22.5

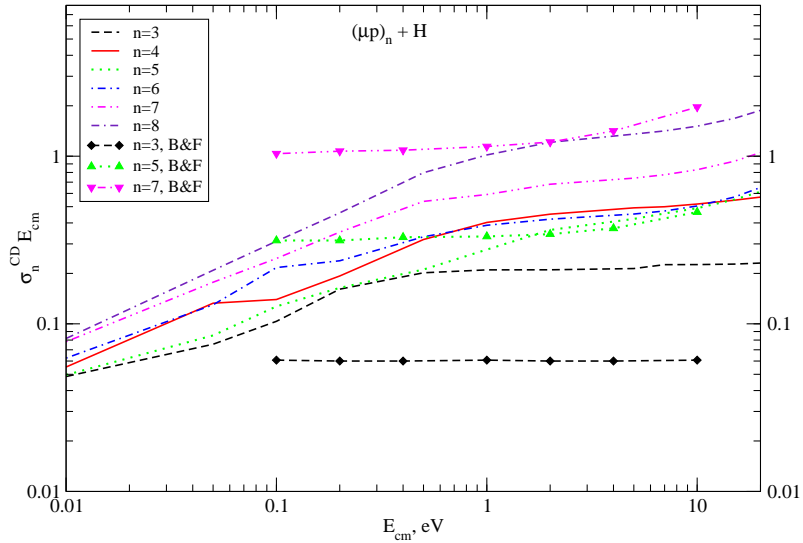


Figure 3: The cross sections of Coulomb deexcitation σ_n^{CD} multiplied by E_{cm} for $(\mu p)_n + H$ collisions calculated in the quantum-mechanical close-coupling method in comparison with the results of Bracci and Fiorentini [11] (B&F).

influence of the open channels with $\Delta n > 1$ which increases for the higher n states and can't be taken into account in the two-state approaches [11-13].

The distribution over the final states n' is completely different from the semiclassical results [11] as illustrated in Fig. 4 and Table 3. The present calculations predict that $\Delta n = 1$ transitions

dominate in agreement with the semiclassical, AAA and CTMC results however the transitions with $\Delta n > 1$ are strongly enhanced as compared to the results [11-13]. To determine the fraction of the transitions with $\Delta n > 1$ in the total CD cross section, the values

$$f_n = \frac{\sigma_n^{\text{CD}} - \sigma_{n,n-1}}{\sigma_n^{\text{CD}}} \cdot 100\%.$$

are also presented.

The calculated CD cross sections $\sigma_{n,n-1}(E)$, $\sigma_n^{\text{CD}}(E)$ and $f_n(E)$ for $(\mu p)_n + H$ collisions with $n = 3 \div 8$ and energies from 0.01 up to 20 eV are presented in Table 3. The observable variations of the CD cross sections with E can be related to the opening of the additional channels with $\Delta n > 1$. The violation of the known in literature [11-13] n -dependence of the CD cross sections is illustrated in Figs. 2 and 3 and in more detail in Table 3. For $n = 4 \div 6$ we observe the essential variations in the CD cross sections in contrast to the two-state calculations [11-13]. In Fig. 3 this effect can be clearer because of the different energy dependence of the CD cross sections for various n . In our opinion the traditional n dependence ($\sigma_n^{\text{CD}} \sim n^\gamma$ with $\gamma \geq 2$) followed from the semiclassical picture can be reached at the relative energies comparable or much more than $\Delta\varepsilon_{n,n-1}$.

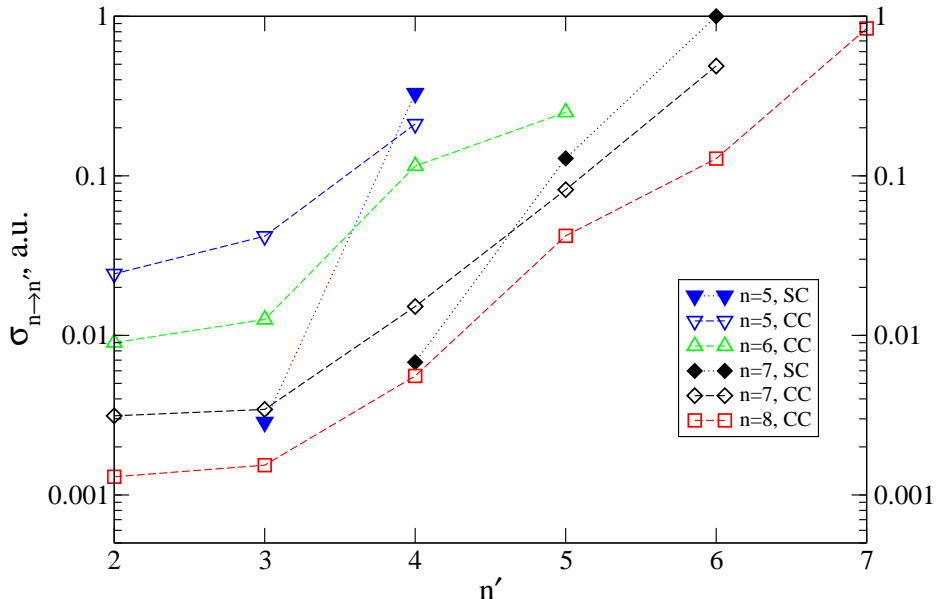


Figure 4: The Coulomb deexcitation cross sections $\sigma_{n,n'}$ in a.u. for $(\mu p)_n + H$ collisions at $E = 1$ eV calculated in the quantum-mechanical close-coupling method in comparison with results of Bracci and Fiorentini [11].

The transitions with $\Delta n = 1$ are most likely but the $\Delta n > 1$ transitions make up a substantial fraction of the total CD cross section (16% - 37%) for $n \geq 4$ in contrast to the two-state approaches [11-13]. The energy dependence of this fraction is completely different for various n . In particular, this behaviour leads to the unexpected dependences of the cross sections on the principle quantum number n and collisional energy E_{cm} .

It is possible that the problem of the high energy fraction of the kinetic energy distribution in the muonic hydrogen is related to the unproper behaviour of the CD cross sections taken in the extended standard cascade model (ESCM) [17] for $n = 3 \div 7$ and based on the semiclassical

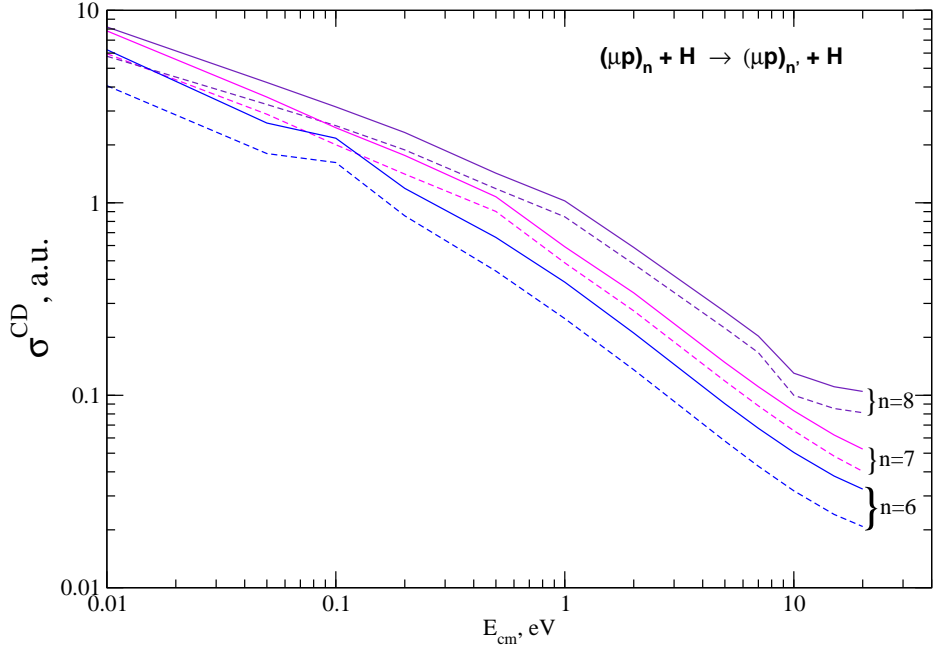


Figure 5: The cross sections of Coulomb deexcitation $\sigma_{n,n-1}$ (dashed) and σ_n^{CD} (solid) in a.u. for $(\mu p)_n + H$ collisions calculated in the quantum-mechanical close-coupling method.

sical model [11]. The dependences of the CD cross sections on n and E used in ESCM are in disagreement with the results of our more elaborate close-coupling consideration.

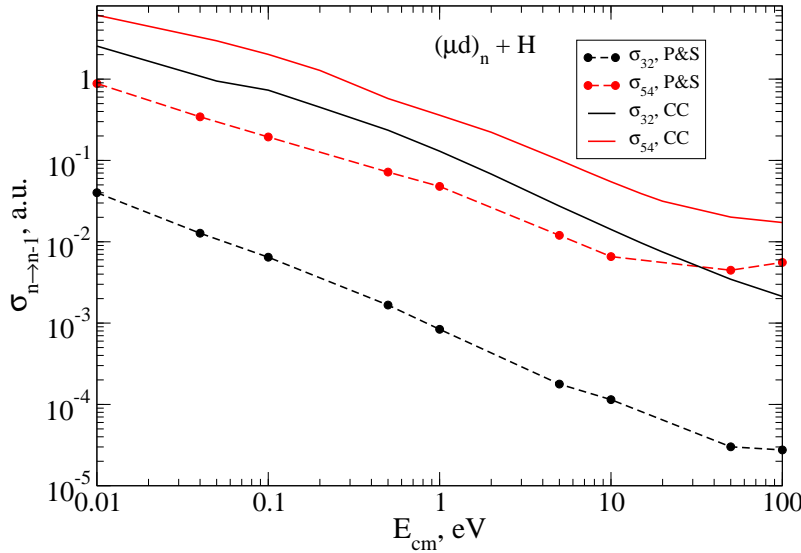


Figure 6: The cross sections of Coulomb deexcitation $\sigma_{n,n-1}$ in a.u. for $(\mu d)_n + H$ collisions calculated in the close-coupling approach (in two-level approximation) (CC) in comparison with results of Ponomarev and Solovyov [13] (P&S).

In Fig. 6 we compare the present cross sections of CD $\sigma_{n,n-1}(E)$ for $(\mu d)_n + H$ collisions with the results of AAA [13] for $n = 3, 5$. As in case of $(\mu p)_n + H$ [11] the transition $3 \rightarrow 2$ is strongly suppressed (almost two order) in comparison with the close-coupling calculations. At the same time for the transition $5 \rightarrow 4$ the results of AAA are only suppressed in four times as compared

with our results. The reason of this discrepancy is not clear at present.

4 Conclusion

The unified treatment of the elastic scattering, Stark transitions and Coulomb deexcitation is presented in *ab initio* quantum-mechanical approach. The main features of the Coulomb deexcitation in the collision of the exotic hydrogen atom in excited states with hydrogen atom have been investigated in detail using the close-coupling method. The new results for the n and E dependences of the CD cross sections are obtained for $n = 3 \div 8$ and relative energies up to 20 eV relevant to the kinetics. The calculated cross sections do not agree with the long-standing traditional beliefs about $\sigma_n^{\text{CD}}(E) \sim n^\gamma/E$ dependence of CD cross sections which is based on semiclassical approximation. The new important results are also obtained for the fraction of the transitions with $\Delta n > 1$. It is shown that the contribution of these transitions is more essential than it is assumed earlier and reaches up to $\sim 37\%$ for $n = 6$. We suppose that our results provide a reliable theoretical input for the further kinetics calculations. More detailed investigations concerning the partial transitions and other exotic particles will be discussed in future publications.

Acknowledgments

We are grateful to Prof. L.Ponomarev for the stimulating interest and the fruitful discussions, to the participants of the Seminar in MUCATEX headed by him for the useful discussions, to T.Jensen and V.Markushin for the sending their data on the CD cross sections for comparison with the present ones and the Russian Foundation for Basic Research (grant No. 03-02-16616) for financial support.

References

- [1] J.F.Crawford et al., Phys.Rev. D **43**, 46 (1991).
- [2] A.Badertscher et al., Phys.Lett. B **392**, 278 (1997).
- [3] M.Leon and H.A.Bethe, Phys.Rev. **127**, 636 (1962).
- [4] T.P.Terrado and R.S. Hayano, Phys.Rev. C **55**, 73, (1977).
- [5] V.P.Popov and V.N.Pomerantsev, Hyp. Interact. **101/102**, 133 (1996).
- [6] V.P.Popov and V.N.Pomerantsev, Hyp. Interact. **119**, 133 (1999).
- [7] V.P.Popov and V.N.Pomerantsev, Hyp. Interact. **119**, 137 (1999).
- [8] V.V.Gusev, V.P.Popov and V.N.Pomerantsev, Hyp. Interact. **119**, 141 (1996).
- [9] T.S.Jensen and V.E.Markushin, PSI-PR-99-32 (1999); nucl-th/0001009.
- [10] T.S.Jensen and V.E.Markushin, Eur.Journ.Phys. D, **19**, 165 (2001).
- [11] L.Bracci and G.Fiorentini, Nuovo Cim. **43A**, 9 (1978).
- [12] A.V. Kravtsov, A.I. Mikhailov, L.I.Ponomarev, E.A.Solovyov, Hyp. Interact. **138**, 99 (2001).

- [13] L.I.Ponomarev and E.A.Solovyov, *Yad.Fiz.* **65**, 1615 (2002).
- [14] E.A.Solovyov, *Uspekhi Fiz. Nauk* **157**, 437 (1989) [Sov. Phys. Usp. **32**,228 (1989)].
- [15] T.S.Jensen and V.E.Markushin, *physics/0205076*; private communication.
- [16] V.N.Pomerantsev and V.P.Popov, unpublished.
- [17] T.S.Jensen and V.E.Markushin, *physics/0205077*.